Pyrazole Functionalized Organo-Ceramic Hybrids for Noble Metal Separations

Jun S. Lee and Lawrence L. Tavlarides
Dept. of Chemical Engineering and Materials Science, Syracuse University, Syracuse, NY 13244

DOI 10.1002/aic.10513
Published online July 13, 2005 in Wiley InterScience (www.interscience.wiley.com).

A series of pyrazole-functional adsorbents is synthesized by sol–gel processing technology and used to study the extraction characteristics for palladium, platinum, and gold chlorides from leaching solutions. An organosilicon compound, N-(trimethoxysilylpropyl)-pyrazole, is synthesized as the functional precursor for these adsorbents. Hydrothermal treatments for the gelled materials alter pore characteristics without chemical property changes. To study adsorptive extraction of Pd(II), Pt(IV), and Au(III) chlorides, the hydrothermally treated adsorbent is used. The experimental results show that this adsorbent has high Pd(II) uptake capacity (1.41 mmol/g), strong selectivity for Pd(II) chloride over Pt(IV) and Au(III) chlorides, and no reactivity for Cu(II) and Fe(II) in 2.0 M HCl solutions. The material also has sustainable stability over repeated metal loading and stripping in a short column. In addition to the experimental studies, the adsorption processes in batch and packed column systems are successfully modeled by using a pore diffusion model and presented. © 2005 American Institute of Chemical Engineers *AIChE J,* 51: 2702–2711, 2005

Keywords: sol-gel synthesis, noble metal separations, palladium, platinum, gold, organo-ceramic adsorbents, adsorption models, adsorbents

Introduction

The mining industry requires efficient and advanced extraction technologies for noble metals because the demand for these metals continues to increase for various applications, although the resources are very limited. Special attention on advanced extraction technologies has also been directed for the recovery and recycling of such metals from industrial wastes, such as spent electronic components and catalysts.[1]

Solvent-extraction processes for noble metal extraction are economically viable because it is possible to achieve highly selective separations and effective enrichments.[2] A variety of organic chelants have been developed for this purpose.[3] These organic chelants have also been immobilized on solid supports such as polymer resins[4] and ceramics[5] as chelating adsorbents for the same purpose. Adsorption processes using these types of materials are favorable alternatives for the recovery of noble metals from dilute leaching solutions.

Recently, our research group has introduced a series of organo-ceramic adsorbents that are synthesized by a sol–gel processing technique for metal extractions.[6-8] These adsorbents generally have significantly high metal uptake capacities, good physicochemical stabilities, and well-defined pore geometries compared to those of other preexisting metal chelating ceramic-based adsorbents.

In this study, pyrazole-functionalized organo-ceramic adsorbents (SOL-PzPs) are synthesized and applied for extraction and separation of palladium (II) [Pd(II)], platinum (IV) [Pt(IV)], and gold (III) [Au(III)] chlorides from HCl solutions. Pyrazole compounds have been considered to be good metal chelants because of the nucleophilicity of nitrogen atoms, different steric accessibility through appropriate substitution, and hydrolytic and thermal stability.[9] Depending on the types of substituted ligands on the pyrazole moiety and the substitution positions, pyrazole-functionalized compounds are characterized by different behaviors in coordination with metal ions.

Correspondence concerning this article should be addressed to L. L. Tavlarides at lltavlar@syr.edu.

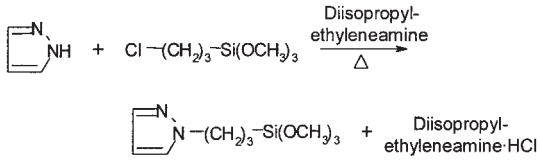

Scheme 1.

Accordingly, these ligands have been used for metal complexations in many applications.[10-12] In particular, pyrazole-functionalized extractants have a good reactivity and selectivity for platinum group metals (PGM) over that of other transition metals.[13-15] For example, du Preez and coworkers[15] reported a series of pyrazole-based extractants for the separation of palladium and platinum in HCl solutions. These extractants have fast extraction kinetics and high selectivity for palladium over platinum in HCl solutions. Even though pyrazole compounds have good properties for noble metal extractions, only a few attempts have been made to incorporate the functionality on solid supports for noble metals[16] and Cu(II), Zn(II), and Cd(II).[17] Thus, there is strong motivation to develop a pyrazole-functional organo-ceramic adsorbent by our sol–gel processing scheme. The results from this study show that SOL–PzPs adsorbents have high potential to be used in noble metal separations such as high uptake capacity and selectivity for Pd(II), no reactivity for Cu(II) and Fe(II), and high physicochemical stability. Examples of target solution are leachated from precious metal ores, which have approximate concentrations of the Pt(IV) $\approx$ [1.5 mmol/L], Pd(II) $\approx$ [6.0 mmol/L], and Au(III) $\approx$ [0.01 mmol/L] in chloride solutions in which Cu(II) and Fe(III) of concentration [5.0 mol/L] and [75 mol/L], respectively, are present.[18,19]

This work describes material synthesis, characterization, and adsorption modeling. The discussion will cover the synthesis of a pyrazole functional precursor silane [*N*-(trimethoxysilylpropyl)-pyrazole]; sol–gel processing to fabricate the adsorbents; effects of posttreatment after gelation on the adsorbent structure and metal complexation; characteristics of the adsorbent for the separation of Pd(II), Pt(IV), and Au(III) chlorides from high-concentration HCl solutions (1–5 mol/L); and development of adsorption models for batch and packed column contacting systems.

Experimental

Synthesis of Precursor and Adsorbent

The functional precursor silane, *N*-(trimethoxysilylpropyl)-pyrazole (PzPs), as shown above, is synthesized by the N-alkylation reaction using equimolar amounts of 1H-pyrazole (Lancaster Co.) and 3-chloropropyltrimethoxysilane (Aldrich Chemical Co.) in the presence of diisopropyl-ethylamine (Aldrich Chemical Co.) as a proton scavenger as shown in Scheme 1. The purity of PzPs used for adsorbent synthesis is >98%, as determined by GC/MS analysis.

SOL-PzPs is synthesized by the two-step condensation scheme as reported in our earlier publications.[6,8] In the first step, both the functional precursor silane (PzPs) and the crosslinking silane [tetraethoxysilane (TEOS); Aldrich Chemical Co.] are independently hydrolyzed and condensed in separate vessels to produce their oligomers. In the second step, the oligomerized silanes are mixed and cocondensed to produce a gel material. After gelation, the material is divided into halves: the first half is aged for 24 h at 25°C (SOL-PzPs-B-18) and the other half is treated hydrothermally (SOL-PzPs-BD-5). In this hydrothermal process, the gel is boiled in 50% v/v acetone and water mixture at 60°C for 12 h, and repeatedly boiled in fresh acetone for 24 h. These gels are dried for an additional 24 h at 80°C and are crushed into particle sizes ranging from 125 to 180 μm for characterization studies, unless otherwise specified.

Characterization

For the characterization study, Pd(II), Pt(IV), and Au(III) chloride solutions are formulated by dissolving potassium tetrachloropalladate (II) (Alfa Aesar Co.), potassium hexachloroplatinate (IV) (Aldrich Chemical Co.), and potassium tetrachloroaurate (III) (Aldrich Chemical) in hydrochloric acid solutions at appropriate concentrations. All other chemicals used in this study are reagent grade.

The metal concentrations are measured with an atomic absorption spectrophotometer (Perkin-Elmer Model 2380) and an ICP-OES (Perkin–Elmer OPTIMA 3300DV). Average pore sizes and surface areas of the adsorbent are measured by nitrogen adsorption at 77 K with Micromeritics ASAP 2000. Carbon and nitrogen contents of synthesized adsorbents are measured by elemental analysis (Oneida Research Services, Whitesboro, NY).

The stability of SOL-PzPs-BD-5 is tested in a 0.8-cm ID column. A 200-mL sample of 4.75 mmol/L Pd(II) chloride solution at 2.0 mol/L HCl concentration is circulated through the column packed with 0.5 g of adsorbent for 24 h at 1.0 mL/min flow rate. After the Pd(II) loading, the column is washed with 10 mL of water and then stripped with 50 mL of 0.5 mol/L thiourea in 0.1 mol/L HCl solution. The stripped column is washed with 0.5 mol/L HCl before the next loading. These loading, stripping, and washing cycles are repeated until desired criteria are satisfied.

Maximum uptake capacities for Pd(II), Pt(IV), and Au(III) chlorides at various HCl concentrations are measured by equilibrating a desired amount of the adsorbent (0.1–0.25 g) with 7–10 mmol/L of the metal chloride solutions at 25°C. For equilibrium adsorption isotherms, desired amounts of the adsorbent are equilibrated with the metal chloride solutions at 2.0 mol/L HCl concentration.

Metal uptake rates of SOL-PzPS-BD-5 are measured for Pd(II) chloride in a batch recycle reactor consisting of a 1.0-cm ID column containing 0.20 g of the adsorbent packed between two layers of 100–120 mesh glass beads. Before contact with the metal solutions, 200 mL of 2.0 mol/L HCl solution is circulated at 10 mL/min flow rate for at least 5 h to ensure complete wetting and protonation of the packed adsorbent. After that, 500 mL of a feed solution in a reservoir is circulated at a desired flow rate, and 2-mL aliquots are taken from the solution reservoir at desired reaction times between 2 and 240 min (nine samples). The change of the solution volume arising from sampling is not compensated for data analysis because only 3.6% of the initial volume of the solution is taken for the analysis of metal concentrations.

Breakthrough experiments are performed with SOL-PzPs-BD-5 for Pd(II), Pt(IV), and Au(III) chlorides. For each breakthrough experiment, 2.0 g of SOL-PzPs-BD-5 are packed in a

Table 1. Physicochemical Characteristics of SOL-PzPs-B-18 and SOL-PzPs-BD-5

Adsorbent	Elemental Analysis		Ligand Density*		Pore Characteristics		
	C (wt %)	N (wt %)	(mmol/g)	$q_{Pd(II)}$** (mmol/g)	D (°A)	SA (m^2/g)	V_P (cm^3/g)
B-18	23.9	9.3	3.3	1.40 ± 0.01	37	124	0.13
BD-5	22.7	8.8	3.1	1.41 ± 0.05	37	437	0.40

*From C and N elemental analyses.
**Palladium uptake capacity at 2.0 mol/L HCl concentration.

0.8-cm ID column. Each feed solution contains approximately 1.0 mmol/L of one of the metal chlorides at 2.0 mol/L HCl concentration. The solutions are passed through the column at 1.0 mL/min flow rate and the effluent solutions are collected fractionally. When the column is saturated, the column is washed with 10 mL of water and stripped with 0.1 mol/L HCl solutions containing 0.5 mol/L thiourea for Pd(II) and Pt(IV) and 0.25 mol/L thiourea for Au(III) by passing at a flow rate of 1.0 mL/min.

In addition to these individual breakthrough experiments, a multimetal breakthrough experiment is performed by using a feed solution containing 0.1 mmol/L each of Pd(II), Pt(IV), and Au(III) chlorides, and 2.5 mmol/L each of copper and iron at 2.0 mol/L HCl concentration. The procedures for metal loading and stripping are the same as those for individual breakthrough experiments.

Results and Discussion

Synthesis of SOL-PzPs adsorbents

The organo-ceramic adsorbents, with and without hydrothermal treatment, SOL-PzPs-BD-5 and SOL-PzPs-B-18, respectively, have different metal uptake capacities, pore characteristics, and adsorption properties, even though these materials are from the same batch. Accordingly, it is of interest to determine how the hydrothermal treatment alters the material properties and adsorption characteristics.

As shown in Table 1, both the carbon and the nitrogen content of SOL-PzPs-B-18 decrease after the hydrothermal treatment (SOL-PzPs-BD-5). This result indicates that the adsorbent structure may be broken down, the unbounded fraction of adsorbent is leached, or both of these occur simultaneously during the treatment. In addition, the increase of pore volume after the treatment supports the loss of part of the adsorbent. However, it is observed that the Pd(II) uptake capacities of SOL-PzPs-B-18 and SOL-PzPs-BD-5 are the same in 2.0 mol/L HCl solutions, regardless of the loss in ligand density.

SOL-PzPs-B-18 and SOL-PzPs-BD-5 also show significantly different behaviors in maximum Pd(II) uptake capacity with respect to HCl concentrations (Figure 1). The Pd(II) uptake capacity of SOL-PzPs-B-18 is the lowest at 0.1 mol/L HCl concentration, increases as the HCl concentration is raised from 0.1 to 2.0 mol/L, and then decreases thereafter. However, the Pd(II) uptake capacity of SOL-PzPs-BD-5 is the highest when HCl concentration is <0.1 mol/L and consistently decreases as the HCl concentration increases. The difference in the uptake capacity at low HCl concentration is possibly caused by either the chemical modification of pyrazole ligands or the change of the pore structure through the posttreatment.

To investigate whether it stems from the modified chemical structure of pyrazole ligands, ^{13}C-CPMAS spectra (Bruker 300 MHz AMX) are taken for fresh, protonated, and Pd(II) loaded adsorbents in 0.1 and 2.0 mol/L HCl solutions (Figure 2). From the spectra for fresh adsorbents, no evidence of chemical modifications of the ligands by the posttreatment, such as ring opening, ligand addition, substitution, and so forth, is found. From the spectra for protonated adsorbents, no differences in acid–base behavior are observed. Peaks for the 3rd and 5th carbons are merged into one peak after a complete protonation in 2.0 mol/L HCl solutions, but these are not merged because of partial protonation at 0.1 mol/L HCl concentrations. When these adsorbents are saturated with palladium chloride at 2.0 mol/L HCl concentration, the 5th carbon peaks from the spectra appear on the left shoulder of the merged peaks. However, the spectrum for SOL-PzPs-B-18 after palladium loading from 0.1 mol/L HCl solutions is different from the spectrum for SOL-PzPs-BD-5 and those spectra for both saturated adsorbents at 2.0 mol/L HCl concentration. This spectral difference after palladium loading is ascribed to the different loading capacity. The lower palladium chloride capacity of SOL-PzPs-B-18 at 0.1 mol/L HCl concentration, we think, originates from the inaccessibility of coagulated and hindered blocks of pyrazole ligands that are generated during the gel formation. These inaccessible blocks at low HCl concentrations are modified and rearranged during the posttreatment and become available for Pd(II) chloride loading as it is observed with SOL-PzPs-BD-5.

From these studies concerning the effects of the posttreatment on the pore structure and adsorption performance of

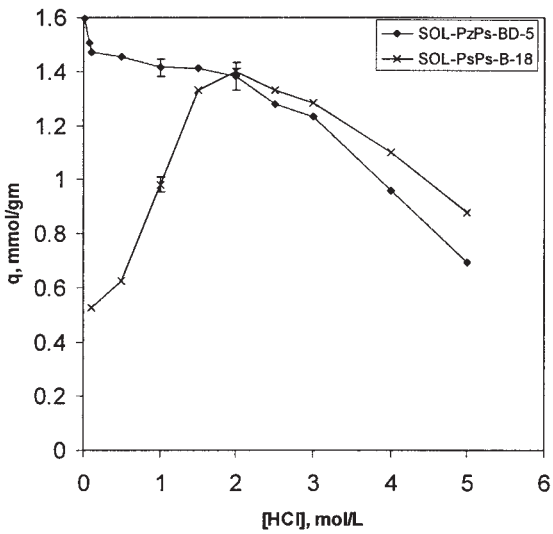

Figure 1. Pd(II) uptake capacities of SOL-PzPs-B-18 and SOL-PzPs-BD-5 at various hydrochloric acid concentrations.

Initial Pd(II) concentration ≈ 7.5 mmol/L; volume of solution = 50 mL; weight of adsorbent = 0.125 g; equilibration time = 24 h.

organo-ceramic adsorbents, it can be concluded that the post-treatment does not modify the chemical structure of the functional ligands, but does modify the pore structure to produce highly porous materials. Consequently, the modified pore structure provides a better adsorption environment to permit high utilization of incorporated pyrazole ligands for the Pd(II) uptake.

Adsorption characterization

SOL-PzPs-BD-5 is used for adsorption of Pd(II), Pt(IV), and Au(III) chlorides from hydrochloric acid solutions because this adsorbent has better material properties than those of SOL-PzPs-B-18. This characterization study includes material stability, adsorption equilibria, Pd(II) uptake kinetics at different adsorbent particle sizes and metal concentrations in a batch recycle reactor, and breakthrough experiments in packed columns.

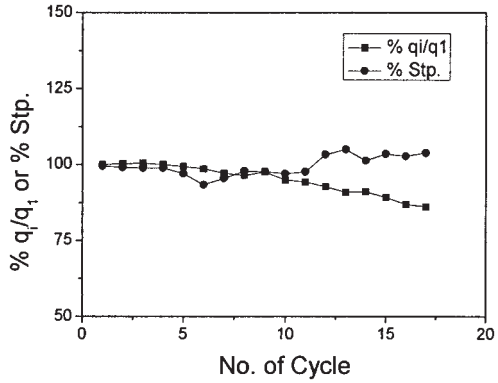

Figure 3. Stability test for SOL-PzPs-BD-5 by repeated Pd(II) loading and stripping cycles.

q_i is Pd(II) uptake capacity at ith cycle; q_1 is the uptake capacity at 1st cycle (1.37 mmol/g).

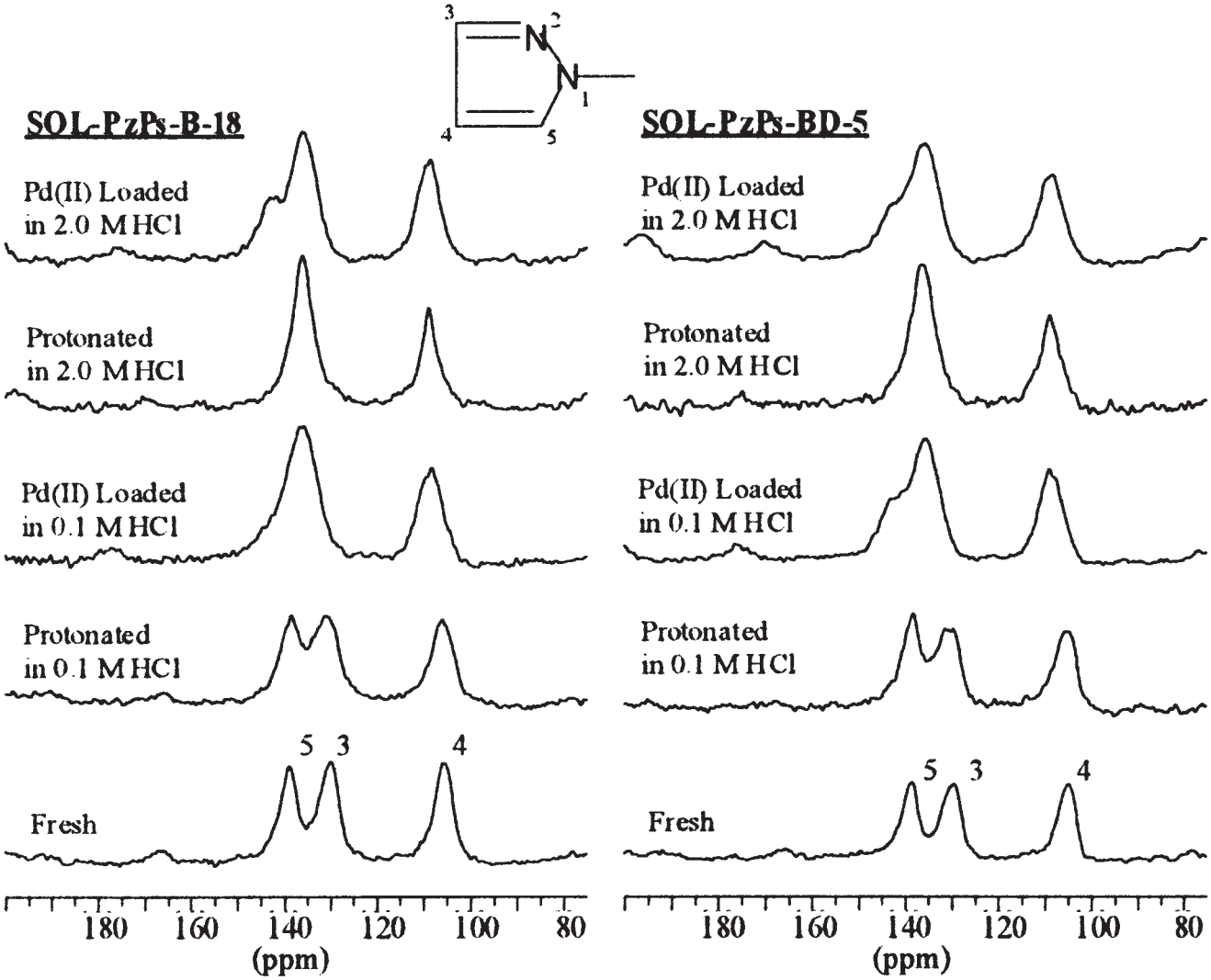

Figure 2. ^{13}C-CPMAS spectra for fresh, protonated, and Pd(II) loaded in 0.1 and 2.0 mol/L HCl solutions.

External reference for carbon chemical shift: glycine carbonyl at 176 ppm.

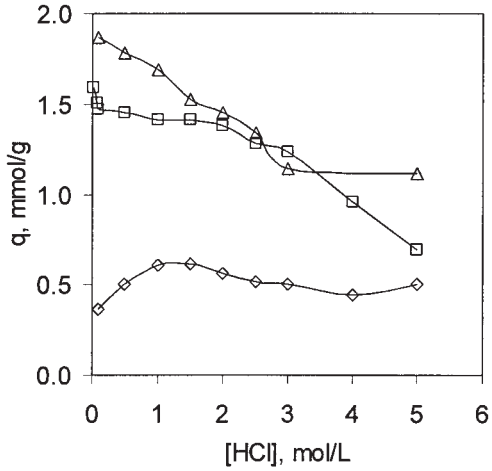

Figure 4. Maximum metal uptake capacities of SOL-PzPs-BD-5 for Pd(II) (□), Pt(IV) (◇), and Au(III) (△) chlorides at various HCl concentrations.

Material stability

Even though the adsorbent has desirable properties such as high metal uptake capacity and fast metal uptake rate, it is important that the material has physicochemical stability for multiple cycles to yield acceptable process economics. Performance of adsorbents declines during repeated use because of oxidation of organic groups, hydrolysis and dissolution of the silica backbone, and irreversible metal binding. Also, sudden contact with stripping agents, which are normally strong and hostile to the adsorbent structure, especially deteriorate the functionality of adsorbents; thus a stability test is performed by successive Pd(II) loading and stripping cycles in a column. The experimental results show that the Pd(II) uptake capacity of SOL-PzPs-BD-5 is maintained at nearly 100% of the original capacity (1.37 mmol/g) for six cycles and decreases to 85% after 17 cycles (Figure 3). The column fails after that as a result of an excessive pressure drop, possibly caused by precipitation of thiourea on the adsorbent and dissolution of silica.[7] Even though the column fails after 17 operations, this study shows that SOL-PzPs-BD-5 has strong operational stability because the degradation occurs primarily during the regeneration processes.

Adsorption in equilibrium

The adsorption reactions of Pd(II), Pt(IV), and Au(III) chlorides with pyrazole functional groups in hydrochloric acid solutions can be represented by the proton-pairing reaction even though the final structures of the complexes of pyrazole–metal chlorides may not have the proton pairing as represented by the following consequent reaction steps.

Protonation of Pyrazole Ligands

$$\overline{RN} + H^+ \leftrightarrow \overline{RNH^+} \qquad (1)$$

where $\overline{RN}$ is the unprotonated pyrazole ligand on the pore surface of the adsorbent, and $\overline{RNH^+}$ is the protonated pyrazole ligand.

Proton-Pairing Reaction

$$MCl_n^{-(n-m)} + (n-m)\overline{RNH^+} \leftrightarrow \overline{MCl_n(RNH)_{n-m}} \qquad (2)$$

where $\overline{MCl_n^{-(n-m)}}$ is $PdCl_4^{2-}$, $PtCl_6^{2-}$, or $AuCl_4^-$ and $\overline{MCl_n(RNH)_{n-m}}$ is the metal complexed pyrazole ligand on pore surface of the adsorbent.

Release of Proton and Chloride

$$\overline{MCl_n(RNH)_{n-m}} \leftrightarrow \overline{MCl_m(RN)_{n-m}} + (n-m)H^+ + (n-m)Cl^- \qquad (3)$$

where $\overline{MCl_m(RN)_{n-m}}$ is the surface metal-pyrazole complex after proton and chloride release.

To investigate whether $PdCl_4^{2-}$, $PtCl_6^{2-}$, and $AuCl_4^-$ follow these reaction steps, maximum metal uptake capacities at different HCl concentrations and equilibrium uptake capacities at different metal concentrations at 2.0 M HCl are measured.

As shown in Figure 4, the maximum uptake capacity for Pd(II) in the HCl concentration range of 0.1–2.0 M is approximately 1.41 ± 0.05 mmol/g, and then it decreases to 0.7 mmol/g at 5 M HCl concentration. The reaction stoichiometry between $PdCl_4^{2-}$ and the protonated pyrazole ligands is expected to be one to two because the metal uptake capacities is approximately half of the ligand density (3.1 mmol/g) in the HCl concentration range of 0.1–2.0 M.

The maximum uptake capacity of Au(III) chloride shows that the capacity rapidly decreases from 1.8 mmol/g at 0.1 M HCl concentration to 1.25 mmol/g at 3.0 M HCl concentration and stays constant thereafter. It is noticed that the maximum Au(III) uptake capacity cannot be determined by our experimental setup in which small amounts (0.1–0.125 g) of adsorbent are contacted with large amounts (100–150 mL) of solutions at high metal concentrations. However, it appears that one Au(III) chloride ion reacts with one protonated pyrazole ligand because the maximum uptake capacity for Au(III) chloride is >1.5 mmol/g and also the extrapolation of adsorption isotherm at 2.0 M HCl concentration for the maximum uptake capacity approaches 2.5 mmol/g (Figure 5).

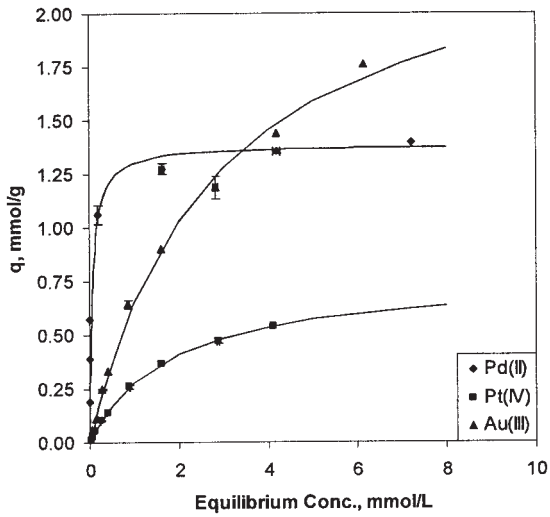

Figure 5. Equilibrium adsorption isotherms of SOL-PzPs-BD-5 for Pd(II) (◆), Pt(IV) (■), and Au(III) (▲) chlorides at [HCl] = 2.0 mol/L.

Table 2. Langmuir Isotherm Constant (K) and Effectiveness Factor (f) for Adsorption Uptake Capacity

Species	K	f
$PdCl_4^{2-}$	15.56 ± 7.91	0.447 ± 0.005
$PtCl_6^{2-}$	0.56 ± 0.17	0.248 ± 0.033
$AuCl_4^-$	0.36 ± 0.04	0.800 ± 0.035

For the adsorption of Pt(IV) chloride, the maximum uptake capacity is <0.7 mmol/g over the entire range of the HCl concentrations studied. Pt(IV) chloride seems to coordinate with four pyrazole ligands such as $[PtCl_2(NR)_4^{2+}]Cl_2$, commonly reported in the literature.[20]

The experimental results for equilibrium uptake capacities of SOL-PzPs-BD-5 in 2.0 M HCl solutions show that this adsorbent has substantially higher Pd(II) uptake capacity than that for Pt(IV) and Au(III) at low metal concentrations (Figure 5). The adsorbent is almost saturated with about 0.2 mmol/L of Pd(II) chloride at equilibrium in the solution but is not completely saturated either by Pt(IV) or Au(III) chlorides even at ≥3 mmol/L metal concentrations. The differences of equilibrium uptake capacities for these three metal chlorides indicate that this adsorbent has a stronger affinity for Pd(II) chloride over Pt(IV) and Au(III) chlorides and provides a utility for almost complete separation of palladium over the others.

Based on the reaction scheme proposed (Eqs. 1–3), the adsorption equilibria between this adsorbent and Pd(II), Pt(IV), and Au(III) chlorides can be described by isotherms with mono-, bi-, and tetra-dentate adsorption mechanisms. However, the mathematical description for the bi- or tetra-dentate adsorption is complicated to use for practical purposes. Thus, it is assumed that Pd(II) and Pt(IV) chlorides form quasi-monodentate complexes with clusters of two and four pyrazole ligands, respectively, whereas one Au(III) chloride ion reacts with one ligand. The assumption of quasi-monodentate adsorption mechanism was successfully used to describe the adsorption of Pd(II) and Pt(IV) chlorides on a functionalized imidazole.[7] The adsorption mechanism (Eq. 2) for Pd(II), Pt(IV), and Au(III) chlorides can be rewritten based on the assumption as

$$MCl_n^{-(n-m)} + \overline{(RNH^+)_{n-m}} \leftrightarrow \overline{MCl_n(RNH)_{n-m}} \qquad (4)$$

where $\overline{(RNH)_{n-m}}$ is considered to be a cluster of $n - m$ number of protonated pyrazole moieties for Pd(II) and Pt(IV) chlorides or a single protonated pyrazole ligand for Au(III) chloride.

The adsorption equilibrium isotherms for these metal chlorides can be described with a modified Langmuir isotherm

$$q_i = \frac{K_i Q f_i C_i}{1 + K_i C_i} \qquad (5)$$

where q_i is the adsorbed amount of metal i (mmol/g); Q is the ligand density (3.1 mmol/g); f_i is the correction factor for actual maximum uptake with respect to the ligand density; K_i is the isotherm constant for metal chloride i; C_i is the concentration of metal i; and i is Pd(II), Pt(IV), or Au(III).

These Langmuir-type adsorption isotherms are fitted to experimental equilibrium data at 2.0 mol/L HCl concentrations to find the isotherm constants (K_i) and the correction parameters (f_i). With the fitting parameters given in Table 2, the experimental equilibrium data are well represented as shown in Figure 5. The correction parameters (f_i) are the ratios of actual maximum uptake capacities with respect to the ligand density. If the adsorption reactions of Pd(II), Pt(IV), and Au(III) chlorides with pyrazole ligands occur as proposed (Eq. 4), the f values should be 0.5, 0.25, and 1.0, respectively. However, the fitted values of f are smaller than these ideal values. These differences between the ideal values and fitted values are attributed to high HCl concentrations in solutions at which the adsorbent interacts not only with these metal chlorides but also free chlorides. The results from this analysis are used for the prediction of the adsorption kinetics in batch and packed columns.

Adsorption kinetics in batch

Among the three metal chloride systems, the Pd(II) chloride system is used to study the adsorption kinetics of SOL-PzPs-BD-5 because this adsorbent has the strongest selectivity for Pd(II) chloride over Pt(IV) and Au(III) chlorides. The experiments are conducted in a batch recycle reactor. By using this type of batch reactor, it is possible to study whether the adsorption kinetics are controlled by pore diffusion or chemical reaction at minimal film mass-transfer resistance. Preliminary experiments at various recycle flow rates indicate that the concentration change of the solution in the vessel is not affected at recycle flow rates > 30 mL/min. Thus, it is assumed that the reactor is operated in the differential mode, and the external mass-transfer resistance is minimized at a flow rate of 40 mL/min (121 bed volume/min).

To determine whether chemical reaction or pore diffusion in the pellet is the adsorption-controlling step, a series of experiments has been conducted at four different adsorbent particle

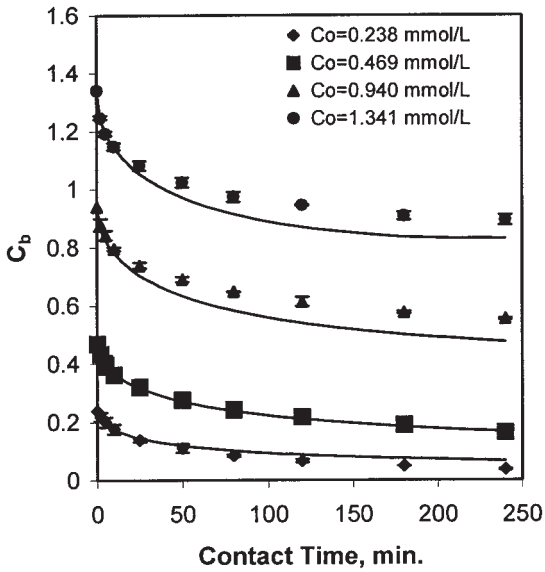

Figure 6. Evolution of Pd(II) concentrations in the reservoir for various initial concentrations.

Adsorbent weight = 0.2 g (125–180 μm); recycle flow rate = 40 mL/min; C_b = Pd(II) concentration measured from the reservoir at given times; solid lines: pore diffusion model ($D_M = 8.33 \times 10^{-6}$ cm^2/s, $\tau = 2.5$).

sizes. The results from these experiments show that the apparent adsorption kinetics is affected by the particle sizes and indicates that the diffusion of Pd(II) chloride ions in pores controls the adsorption process. Thus, a pore diffusion model is developed to predict the adsorption of Pd(II) chloride ions on SOL-PzPs-BD-5.

Accordingly, the following equations along with initial and boundary conditions are used to describe the adsorption kinetics in the batch system.

Macroscopic Mass Balance Equation

$$V_T(c_{b_0} - c_b) = w\bar{q} \tag{6}$$

$$\bar{q} = \frac{3}{R^3}\int_0^R qr^2 dr \tag{7}$$

Pore Diffusion Equation

$$\left(\varepsilon_p + \rho_p \frac{\partial q}{\partial c}\right)\frac{\partial c}{\partial t} = \frac{D_p}{r^2}\frac{\partial}{\partial r}\left(r^2 \frac{\partial c}{\partial t}\right) \tag{8}$$

Initial and Boundary Conditions

$$c = 0 \qquad t \le 0 \qquad 0 \le r \le R \tag{9a}$$

$$\frac{\partial c}{\partial r} = 0 \qquad r = 0 \tag{9b}$$

$$k_f(c_b - c) = D_p \frac{\partial c}{\partial r} \qquad r = R \tag{9c}$$

Here V_T is the reservoir volume (0.5 L) where changes in metal concentrations are measured, w is the mass of adsorbent (0.2 g), $\bar{q}$ is the average concentration of Pd(II) over the entire particle, q is the local equilibrium accumulation at a given time and radial distance from the center of the adsorbent particle, c_b is the concentration of Pd(II) in the reservoir, c_{b_0} is the initial concentration of Pd(II) in the reservoir, c is the Pd(II) concentrations in the adsorbent pore solutions, r is the radial distance from the adsorbent particle center assuming a spherical geometry, ε_p is particle porosity (0.36), ρ_p is the density of a particle (1.03 g/cm^3), and D_p is the pore diffusion coefficient assumed to be independent of metal concentrations.

These equations including the initial and boundary conditions are nondimensionalized, transformed to a set of ordinary differential equations by taking radial finite differences, and solved by the technique of method of lines. In this computation, 100 radial grids for a particle are used for precise prediction of concentration profiles in the pores. Pore diffusion and external mass-transfer coefficients are calculated by using the following correlations.

Assuming that the Crittenden[21] expression applies

$$D_p = \frac{\varepsilon_p D_M}{\tau} \tag{10}$$

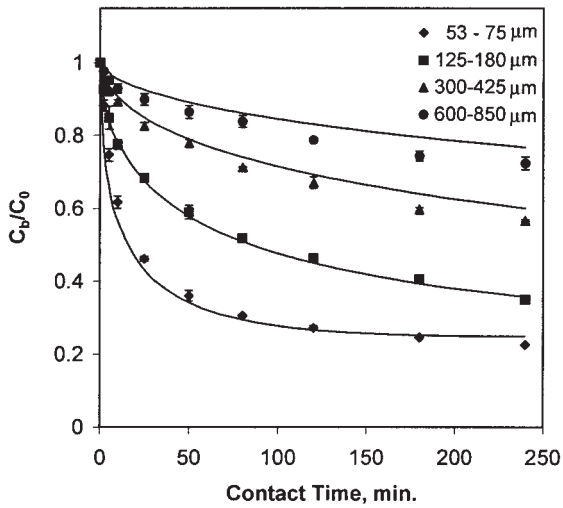

Figure 7. Evolution of Pd(II) concentrations in the reservoir for various particle sizes of SOL-PzPs-BD-5.

Adsorbent weight = 0.2 g; C_0 = 0.473 mmol/L; recycle flow rate = 40 mL/min; C_b = Pd(II) concentration measured from the reservoir at given times; solid lines: pore diffusion model (D_M = 8.33 × 10^{-6} cm^2/s, τ = 2.5).

$$k_f = J_D \frac{u_s}{\mathrm{Sc}^{2/3}} \tag{11}$$

where D_M is the molecular diffusivity of Pd(II) chloride, τ is the tortuosity of the adsorbent, u_s is the fluid superficial velocity (0.85 cm/s), Sc is the Schmidt number, and J_D is the Colburn coefficient evaluated using the correlation given by Wilson and Geankoplis.[22]

D_M and τ are used as fitting parameters because there are no reported values of the molecular diffusion coefficient for Pd(II) chloride in the literature, and τ is an adsorbent-specific property. The optimal values of D_M and τ in this model are determined by minimizing the averaged absolute relative error (AARD), according to the definition shown below, between the calculated bulk concentrations and experimental data for the adsorbent particle size range of 125–180 μm. These values are 8.33 × 10^{-6} cm^2/s and 2.5, respectively. The pore diffusion coefficient (D_p) and external mass-transfer coefficient (k_f) from these values and the above relationships (Eqs. 10 and 11) are 1.20 × 10^{-6} cm^2/s and 1.7 × 10^{-2} cm/s, respectively.

The AARD is defined here as

$$\mathrm{AARD} = \frac{1}{m \cdot n}\sum_1^m \sum_1^n \left|\frac{c_{b,\mathrm{calc}} - c_{b,\mathrm{exp}}}{c_{b,\mathrm{exp}}}\right|_{i,j} \tag{12}$$

where m is the number of initial concentrations studied, n is the number of data points collected in an experiment for an initial concentration, $c_{b,\mathrm{exp}}$ is experimentally measured bulk concentration at a given time and for an initial concentrations, and $c_{b,\mathrm{calc}}$ is the computed concentration by the model at the same condition at which the equivalent experimental data are collected.

This pore diffusion model with the minimal AARD value of 0.09 predicts the experimental data well for this particle size, as shown in Figure 6. In addition, this pore diffusion model

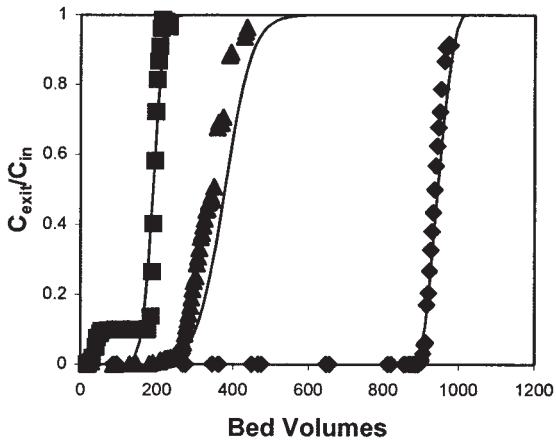

Figure 8. Individual breakthrough curves of SOL-PzPs-BD-5 for Pd (◆), Pt (■), and Au (▲) at 2.0 M HCl concentration.

Adsorbent = 2.0 g (125–180 μm); bed volume = 2.98 mL; flow rate = 1.0–1.1 mL/min; feed concentration (C_{in}) = 1.0 mmol/L; maximum loading = 1.27 mmol Pd/g, 0.28 mmol Pt/g, and 0.50 mmol Au/g; C_{exit}: metal concentrations at column exit; solid line–model prediction.

successfully predicts the overall adsorption kinetics for four different particle size ranges as the predicted results are presented in Figure 7.

Adsorption in packed column

The adsorption behavior of SOL-PzPs-BD-5 in a packed column is studied for Pd(II), Pt(IV), and Au(III) chlorides by performing individual breakthrough experiments at 1.0 mmol/L concentration of each of these metal chlorides in 2.0 mol/L HCl solutions.

The experimental results show that the breakthroughs occur in sequence of Pt(IV), Au(III) and Pd(II), as shown in Figure 8. Two consecutive breakthroughs occur for the platinum chloride system after 25 bed volumes (0.07 L) for which C/C_0 remains at 0.1 until 180 bed volumes (0.54 L) at which the main breakthrough occurs. A similar phenomenon is also observed for the feed concentration of 1.53 mmol/L at 2.0 mol/L HCl concentration, in which case C/C_0 remains at 0.085 before the second breakthrough occurs. The constant leaching of platinum chloride before the main breakthrough indicates that there are other stable chloroplatinum complexes in the solution that are not reactive to pyrazole ligands. Even though spectral studies for this effluent platinum solution have not been performed, likely species are mono-dissociated hydrogenhexachloroplatinate ($HPtCl_6^-$) or hydrolyzed chloroplatinum complexes, as reported by Nachtigall et al. in their ion chromatography study.[23] The breakthrough of Au(III) chloride is less sharp than that of either Pd(II) chloride or Pt(IV) chloride. This broader breakthrough is most likely a result of the longer concentration transition through the column that will be discussed later in the numerical analysis section. A sharp breakthrough of Pd(II) chloride occurs after 900 bed volumes (2.68 L). Substantially large gaps between these breakthroughs show the possibility of complete separation of these noble metal chlorides at moderate concentrations. In addition, the loaded metals can successfully be eluted by using fewer than 15 bed volumes of 0.25–0.5 mol/L thiourea in 0.1 M solutions with high percentage recovery (95–100%).

To predict the breakthrough curve of Pd(II) chloride in the column, the pore diffusion model (Eq. 8) with initial and boundary conditions (Eqs. 9a–9c), parameter correlations, and the Langmuir isotherm (Eq. 5) are coupled and solved with the mass balance equation for the column.

Column Mass Balance Equation:

$$u_s \frac{\partial c_b}{\partial z} + \varepsilon \frac{\partial c_b}{\partial t} + \rho_b \frac{\partial \bar{q}}{\partial t} = 0 \tag{13}$$

$$\frac{\partial \bar{q}}{\partial t} = \frac{3k_f}{R\rho_p}\left(c_b - c\big|_{r=R}\right) \tag{14}$$

$$c_b = 0 \qquad z \geq 0 \qquad \text{and} \qquad t \leq 0 \tag{15a}$$

$$c_b = c_{in} \qquad z = 0 \qquad \text{and} \qquad t > 0 \tag{15b}$$

Here ε is the packed column void fraction ($\varepsilon = 0.33$), ρ_b is the bulk density of the bed ($\rho_b = 0.69$ g/cm^3), R is the average particle radius (1.55×10^{-2} cm), $c\,|_{r=R}$ is the metal concentration at particle outer surface, and c_{in} is the metal concentration in feed solutions.

The method of lines is used to solve both sets of equations simultaneously. In this method, the number of radial grids of a particle and axial grids of the column in the computation are 51 and 125, respectively. Details of the computational technique can be found elsewhere.[24]

This pore diffusion model represents the experimental breakthrough curve for its slope and the breakthrough capacity ($C/C_0 = 1.0$) well by using the diffusivity (D_M) of Pd(II) chloride and the tortuosity (τ) of the adsorbent from the batch kinetics modeling (Figure 8). The calculated capacities for Pd(II) chloride are 1.27, 1.30, and 1.30 mmol/g by the breakthrough experiment, by the pore diffusion model, and by the adsorption isotherm (Eq. 5), respectively.

Further, this model is applied to predict the breakthrough curves of Pt(IV) and Au(III) chlorides by assuming the molecular diffusivities of these metal chlorides are the same as Pd(II) chloride ($D_M = 8.33 \times 10^{-6}$ cm^2/s) with the same tortuosity ($\tau = 2.5$) of adsorbent. Even though the molecular diffusivities of these metals are expected to be different, this prediction test is valuable to investigate the reason for the differences in slopes of breakthrough curves of these metal chlorides.

As noticed from the experimental results, the breakthrough of Au(III) chloride is less sharp than those of Pd(II) and Pt(IV) chlorides. However, the broader breakthrough is not likely because of slower diffusion of Au(III) chloride in the pore, given that the breakthrough of Pt(IV) chloride is sharper than that of Au(III) chloride, even though Pt(IV) chloride has a larger metal complex radius than that of Au(III) chloride. In addition, the pore diffusion model with the same molecular diffusion coefficient can predict breakthrough curves as shown in Figure 8. Therefore, the broader breakthrough is most likely explained by a longer concentration transition through the column that results from less favorable adsorption equilibrium between pyrazole ligands and Au(III) chloride ions. To see how the equilibrium properties—maximum uptake capacities

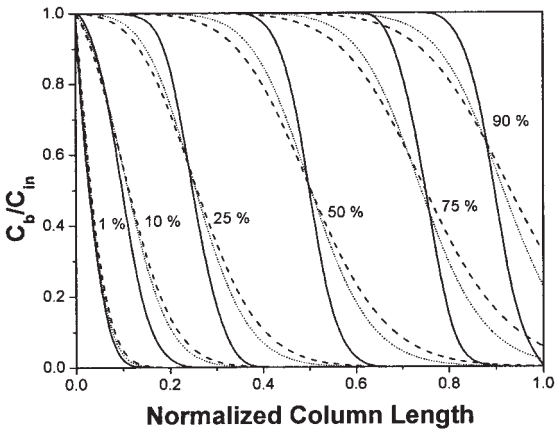

Figure 9. Computed concentration profiles of Pd(II), Pt(IV), and Au(III) chlorides in packed column at various percentages of breakthrough loading capacity of each metal chloride.

C_{in}: feed solution concentration (1.0 mmol/L); C_b: concentration of metal chloride in bulk solution; solid line: Pd(II); dotted line: Pt(IV); and dashed line: Au(III).

and isotherm constants—affect the shape of the concentration profile, the concentrations of Pd(II), Pt(IV), and Au(III) chlorides through the column are computed by using the pore diffusion model at various percentages of the breakthrough loading capacities. Figure 9 shows that the concentration profiles are similar to each other at the beginning of column operation (that is, after 1.0% of loading). However, transitions of concentration profiles of Pt(IV) and Au(III) chlorides become longer, whereas the profile of Pd(II) chloride maintains the same original shape as the column operation is continued. At the near saturation condition (90% of loading), the transition of concentration profile of Au(III) chloride is the longest.

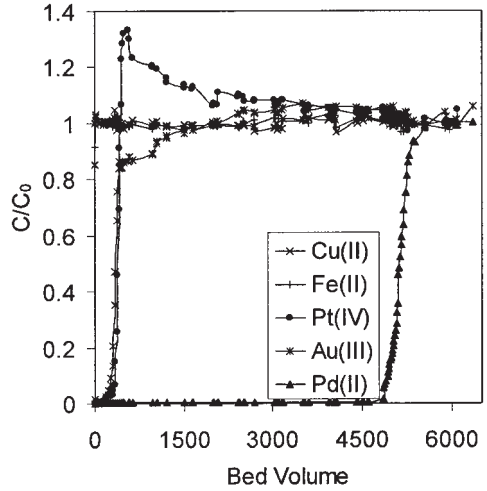

Figure 10. Multimetal breakthrough curves in the column of SOL-PzPs-BD-5 (bed volume = 2.98 mL) in 2.0 mol/L HCl solution.

Flow rate = 1.0–1.1 mL/min; feed solution composition: [Pd(II)], [Pt(IV)], and [Au(III)]: each 0.1 mmol/L; [Cu(II)] and [Fe(II)]: each 2.5 mmol/L; maximum loading = 0.77 mmol Pd/g, 0.00 mmol Pt/g, and 0.03 mmol Au/g.

Multicomponent breakthrough

In addition to individual breakthrough studies, a multimetal breakthrough experiment is performed to demonstrate the capability of SOL-PzPs-BD-5 to extract noble metals from highly concentrated transition metal solutions (Figure 10). The breakthroughs of iron [Fe(II)] and copper [Cu(II)] from the SOL-PzPs-BD-5 column occur immediately after starting the experiment. These immediate breakthroughs indicate that this adsorbent has no reactivity for copper and iron, which are major constituents in noble metal leaching solutions. The breakthroughs of Au(III) and Pt(IV) chlorides occur simultaneously, and then these metals are displaced by the continual adsorption of Pd(II) chloride, which is observed as the dimensionless concentrations (C/C_0) of Au(III) and Pt(IV) exceed 1.0, whereas that of Pd(II) is approximately zero. The displacement of Au(III) and Pt(IV) chlorides by Pd(II) chloride are approximately 44 and 100% (within 300 and 6000 bed volumes), respectively. Thus, only 0.03 mmol/gm of Au(III) is left in the column, whereas 0.77 mmol/g of Pd(II) is loaded after completion of the experiment. Pd(II) uptake capacity of 0.77 mmol/g is approximately the equilibrium loading for the feed concentration. Thus, it is clearly demonstrated that this adsorbent has the strongest affinity for Pd(II) chloride. Further, the adsorption of Pd(II) chloride is not affected by the adsorption of other metals. It is also seen that the affinity for Au(III) chloride is somewhat greater than that for Pt(IV) chloride from the slower displacement of Au(III) chloride than Pt(IV) chloride and complete displacement of Au(III) chloride by Pd(II) chloride does not occur during this adsorption cycle.

After complete saturation of the column, ten bed volumes of 0.5 M thiourea in 0.1 M HCl solution are used to elute the loaded metals. The loaded gold and palladium are recovered with 92 and 100% efficiency, respectively (Figure 11). Only trace amounts of platinum are detected in the eluted solution.

This multimetal breakthrough and elution experiments demonstrate that SOL-PzPs-BD-5 has great potential to extract noble metals from other concentrated metal solutions and to selectively

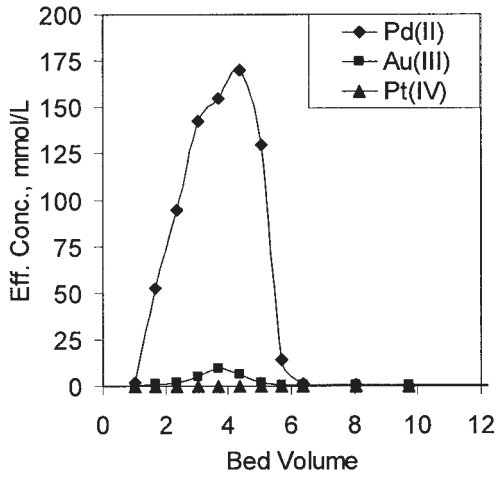

Figure 11. Elution of noble metals from the loaded column of SOL-PzPs-BD-5 (bed volume = 2.98 mL).

Flow rate = 1.0–1.1 mL/min; stripping agent = 0.5 mol/L thiourea in 0.1 mol/L HCl; recovery: Pd(II) = 100%; Au(III) = 92%.

separate palladium from mixture solutions with platinum and gold chlorides at relatively high HCl concentrations (~2.0 M).

Conclusions

The organo-ceramic adsorbents functionalized with pyrazole ligands SOL-PzPs-B-18 and SOL-PzPs-BD-5 are synthesized by sol–gel processing technology for the separation of noble metals at high HCl concentrations. It is shown from this study that an appropriate hydrothermal treatment after gelation can alter pore structures of organo-ceramic adsorbents to give well-developed mesopores and consequently improve adsorption characteristics without sacrificing metal-uptake capacities. An operational stability test for SOL-PzPs-BD-5 shows that this adsorbent has long-term stability over the repeated loading and regeneration in a packed column.

The batch experimental studies for adsorption kinetics show that this adsorbent has rapid adsorption kinetics for Pd(II) chloride uptake. The developed pore diffusion model successfully predicts this rapid adsorption kinetics with the optimized molecular diffusion coefficient (D_M) of Pd(II) chloride and the tortuosity (τ) of adsorbent of values 8.33×10^{-6} cm^2/s and 2.5, respectively. In addition, this model is further developed to predict the breakthrough curve of Pd(II) chloride in a packed column, and the predictions of experimental data are satisfactory. This breakthrough model can also predict the breakthroughs of Pt(IV) and Au(III) chlorides with the same molecular diffusivity of Pd(II) chloride and the tortuosity of the adsorbent, which suggests that the diffusion coefficients for these metal chlorides are not significantly different. It is also shown that the differences in slopes of these breakthrough curves are attributed to adsorption equilibrium properties from the computation of transition concentration profiles.

The applicability of SOL-PzPs-BD-5 adsorbent to a hydrometallurgical separation of noble metals is also demonstrated by performing the multimetal breakthrough experiment with a simulated feed solution. This experiment shows that the adsorbent has no reactivity for copper and iron ions and strong selectivity for Pd(II) chloride over Pt(IV) and Au(III) chlorides. It is also demonstrated from the stripping experiment that the selectively loaded Pd(II) is quantitatively recovered by using an acidic thiourea solution.

All these characterization studies show that this adsorbent has a high potential for application in the separation and recovery of noble metals from leaching solutions of ores, spent catalysts, and disposed microelectronic components. Further investigation is ongoing to selectively recover platinum and gold in copper- and iron-enriched HCl solutions by using other functional ligands. Thus, complete extraction and separation of palladium, platinum, and gold can be achieved with sequential fixed-bed operations.

Acknowledgments

Financial support from the National Science Foundation through Grants CTS-9805118 and CTS-0120204 is gratefully acknowledged.

Literature Cited

1. Kim C-H, Woo SI, Jeon SH. Recovery of platinum-group metals from recycled automotive catalytic converters by carbochlorination. *Ind Eng Chem Res*. 2000;39:1185-1192.
2. O'Sullivan D. Facility recovers metals from spent catalyst. *Chem Eng News.* 1992;Oct. 26:20.
3. Cote B, Benguerel E, Demopoulos GP. Solvent extraction separation of platinum group metals. *Precious Met.* 1993;17:593-617.
4. Sanjiv K, Rakesh V, Venkataramani B, Raju VS, Gangadharan S. Sorption of platinum, palladium, iridium and gold complexes on polyaniline. *Solvent Extr Ion Exc.* 1995;13:1097-1112.
5. D'yachenko NA, Trofimchuk AK, Sukhan VV. Adsorption-photometric determination of palladium using a silica adsorbent modified by *N*-propyl-*N*′-[1-(2-thiobenzothiazole)-2,2′,2′-trichloroethyl]urea groups. *Zh Anal Khim.* 1999;54:151-161.
6. Lee JS, Gomez-Salazar S, Tavlarides LL. Synthesis of thiol functionalized organo-ceramic adsorbent by sol–gel technology. *React Funct Polym.* 2001;49:159-172.
7. Lee JS, Tavlarides LL. Application of organo-ceramic adsorbents functionalized with imidazole for noble metal separations. *Solvent Extr Ion Exc.* 2002;20:407-427.
8. Tavlarides LL, Deorkar NV, Lee JS. High performance adsorbent ceramic compositions synthesized by sol-gel method. U.S. Patent Application No. 09/573 304; 2000.
9. Trofimenko S. The coordination chemistry of pyrazole-derived ligands. *Chem Rev.* 1972;72:487-509.
10. Grotjahn DB, Combs D, Van S, Aguirre G, Ortega F. Synthesis and structure of isomeric palladium(II)–pyrazole chelate complexes with and without an N–H group as hydrogen bond donor. *Inorg Chem.* 2000;39:2080-2086.
11. Saha N, Bhattacharyya D, Kar SK. Model complexes of palladium(II) and platinum(II) with pyrazole- and pyrimidine-derived ligands of biological interest. *Inorg Chim Acta.* 1982;67:L37-L38.
12. Govind B, Satyanarayana T, Veera Reddy K. Platinum metal complexes with some new bifunctional ligands—I. Pyrazole amide complexes with Pd(II) and Pt(II). *Polyhedron.* 1996;15:1009-1022.
13. Pronin VA, Usol'tseva MV, Shastina EN, Volkov AN, Seraya VI. Extraction of Pt(IV), Pd(II), Au(III), and Ag(I) from hydrochloric acid solutions by 3(5)-methylpyrazole. *Zh Neorg Khim.* 1974;19:800-802.
14. Pronin VA, Usol'tseva MV, Shastina EN, Volkov AN, Sokolyanskaya LV. Extraction of palladium and rhodium with N-alkylpyrazoles from hydrochloric acid solutions. *Zh Anal Khim.* 1976;31:1767-1769.
15. du Preez JGH, Knoetze SE, Ravindran S. Nitrogen reagents in metal ion separation. Part X. The separation of palladium from platinum in hydrochloric acid solution by pyrazole derivatives. *Solvent Extr Ion Exc.* 1999;17:317-332.
16. Antokol'skaya II, Myasoedova GV, Bol'shakova LI, Ezernitskaya MG, Volynets MP, Karyakin AV, Savin SB. Concentration and separation of the elements on chelate sorbents. Sorbent for the noble metals based on a styrene–(3)-5-methylpyrazole copolymer. *Zh Anal Khim.* 1976;31:742-745.
17. van Berkel PM, Driessen WL, Reedijk J, Sherrington DC, Zitsmanis A. Metal-ion binding affinity of azole-modified oxirane and thiirane resins. *React Funct Polym.* 1995;27:15-28.
18. DocCopper. Leaching of gold: A technology review of lixiviants. *DocCopper's Gold Prospecting Pages*. 1999 (may be accessed at doccopper@yahoo.com).
19. Mhaske AA, Dhadke PM. Extraction separation studies of Rh, Pt and Pd using Cyanex 921 in toluene—A possible application to recovery from spent catalysts. *Hydrometallurgy.* 2001;61:143-150.
20. Kukushkin YN, Strizhev EF, Krasnov BA, Kiseleva NPK. Equilibria in aqueous solutions of tetramineplatinum(IV) chlorides. *Russ J Inorg Chem.* 1973;18:1144-1146.
21. Crittenden JC, Webber J Jr. Predictive model for design of fixed-bed adsorbers: Parameter estimation and model development. *J Environ Eng Div.* 1978;13685.
22. Wilson EJ, Geankoplis CJ. Liquid mass transfer at very low Reynolds number in packed beds. *I&EC Fundam.* 1966;5:9-14.
23. Nachtigall D, Artelt S, Wunsch G. Speciation of platinum-chloro complexes and their hydrolysis products by ion chromatography. Determination of platinum oxidation states. *J Chromatogr A.* 1997;775:197-210.
24. Gomez-Salazar S, Lee JS, Heydweiller JC, Tavlarides LL. Analysis of cadmium adsorption on novel organo-ceramic adsorbents with a thiol functionality. *Ind Eng Chem Res.* 2003;42:3403-3412.

Manuscript received Oct. 8, 2003, and revision received Feb. 7, 2005.